Heliyon 8 (2022) e10175

Contents lists available at ScienceDirect

Heliyon

journal homepage: www.cell.com/heliyon

Research article

Finasteride-loaded nano-lipidic carriers for follicular drug delivery: preformulation screening and Box-Behnken experimental design for optimization of variables

Shweta Ramkar, Preeti K. Suresh *

University Institute of Pharmacy, Pt. Ravishankar Shukla University, Raipur, Chhattisgarh, 492010, India

ARTICLE INFO

Keywords:
Quality-by-design
Response surface methodology
Nanomedicine
Lipidic carriers
Follicular
Transfollicular
Optimization

ABSTRACT

Finasteride (FIN), a 5-α reductase enzyme inhibitor is mainly used orally for the treatment of androgenic alopecia and benign prostate hyperplasia. The present study was undertaken for systematic optimization and assessment of the designed nanostructured lipid carriers (NLC) to enhance follicular delivery of FIN by topical administration. The NLCs were prepared by microemulsion method, by employing a 3^3 Box-Behnken design and subsequently confirmed by ANOVA analysis. Compritol ATO-888 and Fenugreek oil were selected as the solid lipid and liquid lipid respectively for the fabrication of NLCs. The formulations were characterized for particle size, zeta potential, entrapment efficiency, storage stability and *in vitro* drug release profile. Morphological profile of the NLCs nanocarriers was studied by transmission electron microscopy (TEM). The Fourier Transform Infrared Spectroscopy (FT-IR) spectrum and differential scanning calorimetry (DSC) thermogram demonstrated that FIN entrapment within NLCs was devoid of chemical interaction with the components. The prepared NLCs had satisfactory particle dimensions, zeta potential and entrapment efficiency. The numerical optimization process indicated the optimal NLC composition with 3 mg of SPC, 6 mg lipid and 5 mg of drug. NLCs loaded with FIN had acceptable particle size at 379.8 nm, zeta potential of −37.1 mV and an entrapment efficiency of 84%. Transmission electron microscopy indicated the spherical morphology. *In vitro* release profile indicated a fast initial release and subsequently a prolonged release of FIN from the carrier for 24 h. The release kinetics data displayed a Higuchi diffusion release model with the best match R^2 value (0.848). Short-term stability tests conducted over 4 weeks at 6° and 25 °C demonstrated that the formulation could retain their initial properties during the test period.

1. Introduction

Androgenic alopecia is a chronic and progressive disorder affecting millions and has substantial cosmetic and psychosocial implications. The hormone testosterone plays a crucial role in androgenic alopecia, independent of genetic predisposition [1, 2]. Androgenic alopecia is androgen hormone dependent follicular miniaturization with a patterned hair loss, mainly caused by the dihydrotestosterone (DHT) hormone hydrolysed by 5-α reductase enzyme. Type-II 5-α reductase, the enzyme involved in the conversion of testosterone to DHT is expressed in androgen dependent tissues, in general and hair follicles, in particular and is reported to be critical in androgenic alopecia [3]. Limited treatment modalities are available for androgenic alopecia and this is further limited by the serious systemic side-effects of the available drugs viz., finasteride and minoxidil. In the peripheral conversion of testosterone to DHT, Finasteride (N-(1, 1-dimethyl ethyl)-3-oxo–4-aza-5-androst -1-ene-17-carboxamide), a synthetic 4-azasteroid compound, serves as a specific and competitive inhibitor leading to reduction of the DHT level in prostate gland, hair and liver [4]. It is approved to be administered orally for treatment of benign prostatic hyperplasia or prostate cancer and androgenic alopecia [5, 6]. But the major cause of concern is that on chronic use, several sexual functions related adverse events are reported that ultimately lead to compromised patient compliance [7]. The adverse events of finasteride can be greatly reduced or even completely evaded by exploiting the percutaneous approach for drug delivery to confine the drug action on the scalp [8, 9]. But the low aqueous solubility (11.7 mg L^{-1}) can be a major challenge in transport of finasteride (FIN) across the skin [10]. Nanocarriers have been reported to have the capacity to improve the pharmacokinetics and viability at the targeted location, indicating their value in the current context. Among the various

* Corresponding author.
E-mail address: suresh.preeti@gmail.com (P.K. Suresh).

https://doi.org/10.1016/j.heliyon.2022.e10175
Received 27 March 2022; Received in revised form 18 June 2022; Accepted 29 July 2022

nanocarriers, lipidic nanocarriers offer numerous potential benefits like fewer systemic adverse effects, increased solubility and greater follicular permeability [11, 12]. The levels of sebum is high within the follicular ducts boundaries. The existence of sebum, with its lipophilic character, therefore permits ready interaction with the lipid-based nanocarriers [13, 14].

Transdermal film loaded with drug microplates for FIN delivery and an enhancement in aqueous solubility and skin permeation has been reported [15]. Chitosan decorated FIN nanosystems were synthesised for delivery via skin and the developed systems displayed suitable *in vitro* drug release profile, skin retention characteristics and *ex vivo* performance [16]. FIN loaded microemulsions with increased permeability of the skin to FIN has also been demonstrated [17]. Gel formulations based on propylene glycol, Tween 80 and sodium lauryl sulphate displayed 6-fold increment cumulative FIN release, flux, partition coefficient, input rate, lag time and diffusion coefficient [18].

Quality by design (QbD) is a tried and tested systemic method that can be applied during the preliminary stages of formulation development, designing and optimization to establish the association between various independent and dependent variables that can be instrumental in achieving qualitative uniformity in products. This approach helps in analysing the consequences of critical process parameter on critical quality attributes. In the current study Box Behnken factorial design was implemented to study the influence of the formulation composition in the FIN loaded nano lipidic carriers to achieve the quality target profile with minimal experimental runs [19, 20]. The formulations were prepared by the microemulsion method and were characterised for their morphological features, size, zeta potential, drug entrapment efficiency, and *in vitro* drug release profile.

2. Materials and methods

2.1. Materials

The drug finasteride (FIN) was provided by Cipla Ltd., Mumbai, India. Fenugreek oil was purchased from Parvati Gramodyog Herbal Product, Faridabad, India. Compritol ATO-888 and Soya phosphatidylcholine (SPC) were acquired from Molychem, Mumbai, India. Methanol, ethanol, chloroform and n-octanol were procured from Rankem, Thane, India. All other reagents, solvents and chemicals used in the experiments were of analytical grade.

2.2. Experimental design

For maximizing the experimental efficiency, 3-level, 3-factor Box–Behnken design was used in the study. Using this method, minimal numbers of experiments were required to optimize preparation of NLCs [19, 21, 22]. The NLCs were formulated by microemulsion method and the influence of independent variables on dependent variables was studied [23]. Independent variables in the present study were amount of FIN (X_1), amount of surfactant (X_2) and amount of solid lipid (X_3). Other constraints, i.e., amount of liquid lipid, stirring rate and time, final volume, were kept at fixed levels. The dependent variables selected were mean particles size (Y_1), zeta potential (Y_2) and encapsulation efficiency (Y_3). The lower (−1), medium (0) and higher (+1) values for each factor were selected on the basis of literature survey [12, 24, 25]. The data analysis was performed by ANOVA.

The polynomial equation generated from the experimental design was as follows:

$$Y = b_0 + b_1X_1 + b_2X_2 + b_3X_3 + b_{12}X_1X_2 + b_{13}X_1X_3 + b_{23}X_2X_3 + b_{11}{X_1}^2 + b_{22}{X_2}^2 + b_{33}{X_3}^2$$

where Y is the dependent variable, b_0 is the intercept, X_1, X_2, X_3 are the coded levels of various independent variables, and b_1 to b_{33} are the regression coefficients computed through the experimental values observed for Y. The terms X_1X_2 and Xi^2 (i = 1, 2 or 3) indicate the interaction and quadratic terms, respectively. The statistical validation of the polynomial equation was conducted with ANOVA, by statistical significance of coefficients and r^2 values. The p values ≤ 0.05 were considered statistically significant [23].

2.3. Preparation of NLCs

Finasteride laden NLCs were fabricated by microemulsion method. The mixture of solid lipid (Compritol ATO-888) and liquid lipid (Fenugreek oil) 7 ml were heated at 80 °C [26], and then FIN was added to this lipid mixture. At the same temperature, aqueous phase was heated with surfactant (SPC). By maintaining the temperature, lipid mixture was added slowly to the aqueous phase under continuous stirring at 2000 rpm for a period of 30 min. Preparation was filtered. The microemulsion was quickly added to cold water (0–4 °C), in the ratio of 1:50, forming an NLC dispersion system [27]. The various steps in the preparation of NLCs are presented schematically in Figure 1.

2.4. Optimization and validation

STATISTICA 10 was used for graphical and numerical analysis to determine the best values (Table 1) for the variables based on the desirability criteria. For the evaluation of the selected experimental domain and polynomial equations, the optimum variables were utilised to build a preliminary NLC formulation and the predicted error was compared to the predicted values.

2.5. Characterization of NLC

2.5.1. Thermal analysis

The pure components and the developed NLCs were characterised for the melting point and crystallization behaviour by differential scanning calorimetry (DSC) (Mettler Toledo, DSC 822, Switzerland). Samples (approx. 5 mg) were placed in an aluminium pan and pierced, and the pans were subjected to heating at a scanning rate of 10 °C/min from 20° to 210 °C under nitrogen purge 30 ml/min and in the experiments, empty aluminum pan served as reference standard.

2.5.2. Fourier Transform Infrared (FT-IR) spectroscopy

The IR spectrum of NLC formulations and pure components were examined by Fourier Transform Infrared (FT-IR) spectrometer (Avatar, 370 FT-IR, Thermo Nicolet, USA) utilising KBr pellets at room temperature in order to discover probable interactions that may occur during NLC formation. Samples were prepared by combining with KBr and the mixture were compacted to form a thin pellet. These pellets were measured in the range of 4000 to 400 cm^{-1}.

2.6. Particle size, polydispersity and zeta potential analysis

The particle size (PS), polydispersity index (PDI) and zeta potential (ZP) of the NLC dispersions were determined by photon correlation spectroscopy (Zetasizer Nano ZS, Malvern PCS Instruments, UK). Surface charge of NLCs may influence the interaction and permeation of the formulation. Negatively charged and neutral formulations prefer to co-localize within the skin [28, 29, 30]. The samples were diluted to 1:100 with distilled water before measurement to get a suitable kilo counts per second (kcps). The analyses were conducted with a fixed light incidence angle of 90° at 25 °C.

2.7. Morphological properties

The NLC formulations were analyzed by transmission electron microscopy (TEM) (TEM Jeol JEM-1400). One drop of NLC dispersion was placed over a grid followed by negative staining with uranyl acetate and

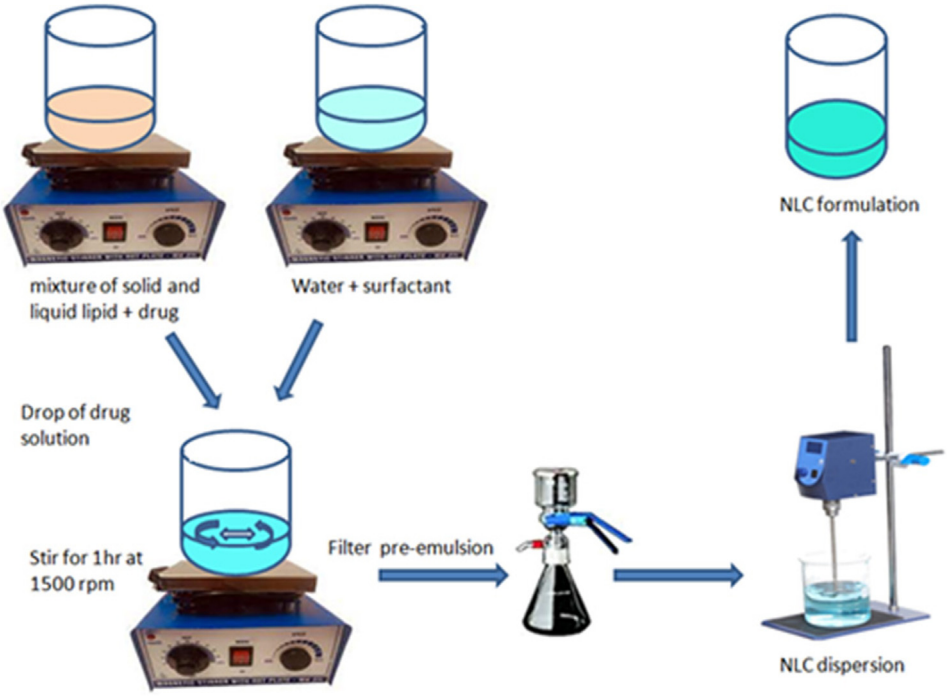

Figure 1. Schematic representation of NLCs formulation.

Table 1. Independent variables and the coded levels of the Box–Behnken design.

Factors	Coded levels		
Independent variables	Low Level (−1)	Medium Level (0)	High Level (+1)
X_1= amount of drug (mg)	1	3	5
X_2= amount of surfactant (mg)	25	50	75
X_3= amount of solid lipid (ml)	3	6	9
Dependent variables	Constraints		
Y_1 = mean particle size (PS)	Minimum		
Y_2 = zeta potential (ZP)	Minimum		
Y_3 = encapsulation efficiency (EE)	Maximum		

Note: X_1, X_2 and X_3 denote independent variables and Y_1, Y_2, Y_3 denote dependent variables.

operated at an accelerating voltage of 60 kV to take the transmission electron photomicrographs of the samples.

2.8. Entrapment efficiency (EE)

The entrapment efficiency (EE) of FIN within NLCs was measured by the method previously reported with some modifications [31]. The EE was calculated by determining the amount of free FIN in NLCs. 0.5 ml of prepared formulation was accurately measured and 10 ml methanol was added as an extracting solvent for the free FIN. The obtained mixture was agitated and centrifuged for 5 min at 1000 rpm (Sigma, 3-30K; Germany). Supernatant having free FIN in methanol, was separated and analysed spectrophotometrically (UV spectrophotometer (UV-1800 Shimadzu, Japan)) to quantify the drug at 219 nm wavelength with FIN-free NLCs serving as blank. The EE was calculated by:

$$\%\mathbf{EE} = \mathbf{W_{total}} - \mathbf{W_F}/\mathbf{W_{total}} * \mathbf{100} \quad (1)$$

Where W_{total} is weight of FIN and lipid in the NLC dispersion and W_F is amount of free FIN measured in the supernatant. All the experiments for measuring EE were performed in triplicate.

2.9. In vitro *drug release study*

The *in vitro* drug release profile of optimized FIN loaded NLC formulation was studied over 24 h using modified Franz-type diffusion cells (diffusion area = 1.3 cm^2) mounted with egg membrane to separate donor and receptor compartments. A defined amount of formulation (equivalent to 5 mg of drug) was introduced into the donor compartment, while the receptor compartment contained 15 mL of phosphate buffer saline (pH 6.5) with 0.8% tween 80 to ensure the sink conditions. The system was placed under stirring rate of 300 rpm and since the NLCs are proposed for topical application, the temperature was maintained at 32 °C to simulate the skin surface. At designated time intervals (1, 2, 3, 4, 5, 6, 7 and 24 h), 1 ml of medium was withdrawn and analysed spectrophotometrically. Each withdrawn sample was replaced with the same volume of fresh PBS solution, so as to maintain the sink conditions.

2.10. Stability study

The physical stability profile of NLC was determined at 6 ± 2 °C and 25 ± 1 °C. The formulations were placed in glass vials for a month at these temperatures and examined on the day of formulation and subsequently 1, 2, 3 and 4 weeks of storage. The samples were analysed for the particle size, PDI and zeta-potential and compared with the fresh NLC formulations [32].

2.11. Statistical analysis

The experimental results of the study were expressed as mean ± standard deviation (SD). The statistical significance of the data set was assessed by unpaired Student t-test for comparing the two experimental groups. A p-value <0.05 was considered as statistically significant in the present study.

3. Results and discussion

3.1. Preparation of NLCs

The preparation of FIN loaded NLCs by microemulsion method was successful. FIN was solubilized in Compritol ATO 888 and fenugreek oil

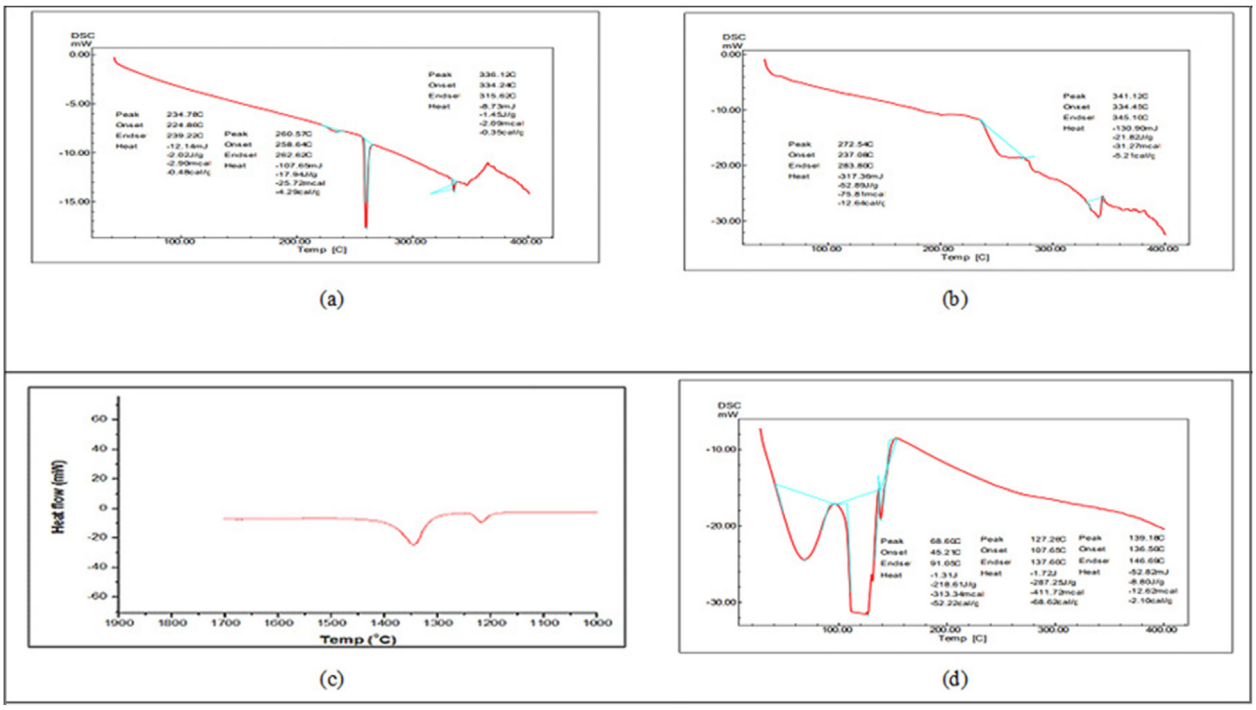

Figure 2. DSC thermograms of FIN (a), Soyalecithin (b), Compitrol ATO 888 (c) and FIN loaded NLC (d).

and no drug residues were observed. For the present study the solid lipid Compritol ATO 888 was selected owing to its melting range above normal body temperature and better solubility profile. In addition to its capacity to solubilise lipophilic drugs, Compritol ATO 888 is also reported to have minimal cytotoxicity [17]. As the liquid lipid, fenugreek oil was selected owing to its beneficial effects on hair [33]. Soya lecithin was chosen as the lipophilic surfactant in the formulation for topical applications due to its well-known characteristics in terms of safety, biocompatibility and acceptable regulatory status and it has also been successfully used in the design of NLCs [34].

3.2. Physicochemical characterization

3.2.1. Thermal analysis

The DSC thermograms of pure FIN, Compitrol ATO 888, Soyalecihin and FIN loaded NLC are presented in Figure 2. Pure FIN displayed a

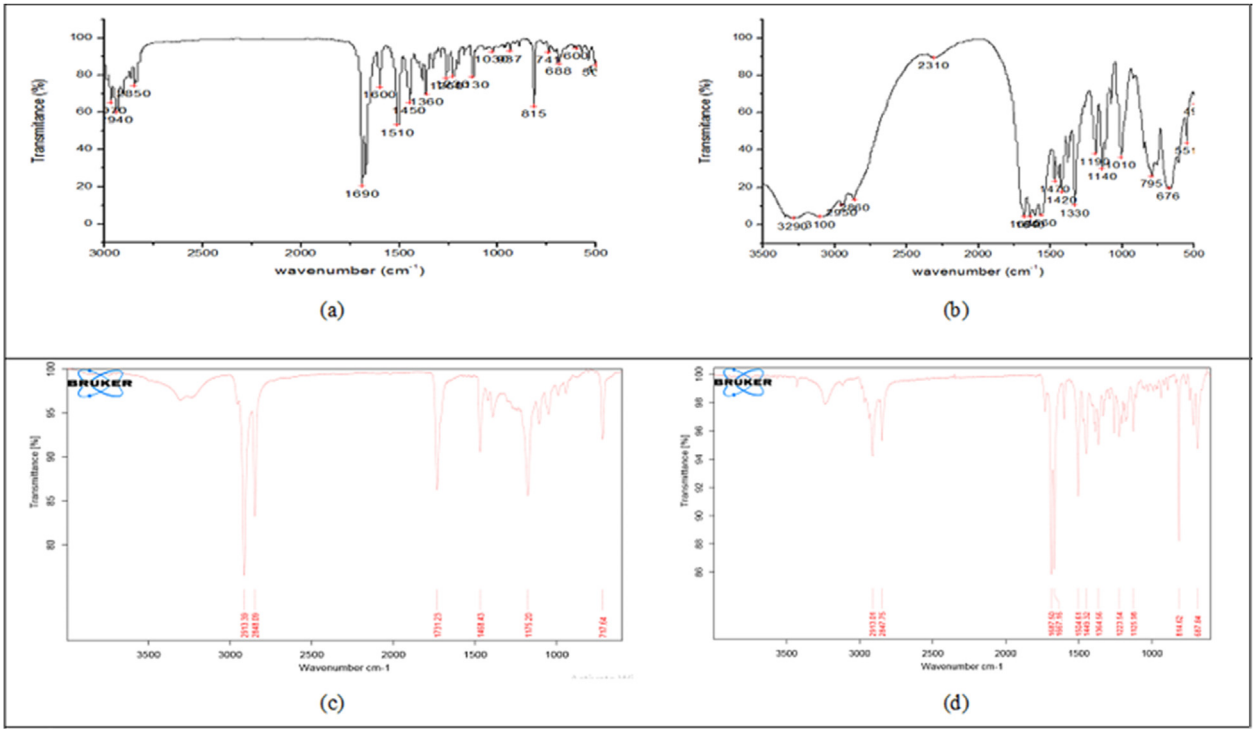

Figure 3. FT-IR spectra of FIN (a), Soyalecithin (b), Compitrol ATO 888 (c), FIN loaded NLC (d).

Table 2. Interpretation of IR spectra of pure drug FIN.

S.No.	Frequency range (cm^{-1})	Functional group
1.	1693	amide group
2	1365	tert-butyl group
3.	3428.45	N–H group
4.	3026	C–H group
5.	1647	C=C group
6.	1749	C=O group

strong endothermic peak at 258.64 °C correlating to its melting point, demonstrating its distinctive crystalline form. Thermogram of phospholipids demonstrated three obviously distinguishable forms of endotherm. The initial endotherm at 237.08 °C was modest, indicated the creation of this peak to movements of the polar portion of the phospholipid molecule. The next strong endotherm peak exhibited at 272 and 283.8 °C might be generated due to the phase transition from a gel-like state to a liquid-crystal state, and it may undergo melting, isomeric or crystal modifications on carbon-chain in the phospholipid [35]. It is obvious from comparison of the DSC curves that FIN and phospholipids display various interactions, such as the creation of hydrogen bonds and Van der Waals forces. The combination of the polar parts of FIN and phospholipids, facilitates the free rotation of the carbon–hydrogen chain in the phospholipids and enclose the polar fractions of the phospholipid molecule, and produce a chronological reduction between the phospholipid aliphatic hydrocarbon chains while the second endothermic peak of the phospholipid vanished, and the phase transition temperature was condensed [36, 37]. In the DSC thermogram of FIN loaded NLC, decreased endotherm peaks at 150 °C of phospholipid was achieved. In the DSC, FIN alone exhibited a significant peak at 258.64 °C. However, in the formulation this peak was noticed as displaced blunt curve at 105.97 °C owing to the presence of liquid and solid lipids and exothermic combination with water to create substantial heat. The typical endothermic peak of Compritol ATO 888 (72.07 °C) was visible in the physical mixture of FIN with excipients of NLC, corroborating the crystallinity of Compritol ATO 888 and its β′ form. The NLC formulation also displayed a diminution in peak intensity of Compritol ATO 888 with a minor shift of the endothermic peak to the lower temperature (70.88 °C) [38].

3.2.2. Infrared spectroscopy

Infrared spectroscopy examination was undertaken for identification of probable interactions between components during fabrication of NLCs [26, 39]. FTIR spectra of pure FIN, soya lecithin, compitrol ATO 888, and optimal FIN loaded NLC are presented in Figure 3. FIN IR spectra exhibited distinctive peaks at 1690 and 1600 cm^{-1} corresponding to the two amide groups. The interpretation of IR spectrum of pure FIN is presented in Table 2. Other peak at 1360 cm^{-1} related to tert-butyl group [36, 40, 41, 42], soya lecithin displayed a broad peak at 2310, sharp peak at 2950, as well as other sharp peaks less than 1800 cm^{-1}. FT-IR spectra of FIN loaded NLC demonstrated elimination of all other peaks rather than 1690 and 1600 cm^{-1} corresponding to the two amide groups moved towards 1687.50 and 1667.16 and two corresponding peaks of soya lecithin 2913.01 and 2847.75 cm^{-1} also existed. 1731.23 cm^{-1} was found on the compitrol ATO 888. These findings are indicators of mild physical interactions between FIN and soyalecithin that might have taken place during the NLC formation.

3.3. Data analysis and formulation optimization

In the Box–Behnken design for experimental design and process optimization, three elements and three levels were considered. The response surface randomised design provides 17 runs with various combinations of the specified elements, including 5 runs with centre points for which responses were gathered and assessed (Table 3). Quadratic polynominal models were determined to offer the greatest match for all the three criteria. The model terms revealed that independent factors had a direct influence on dependent variables (responses). To discover the ideal experimental parameter, all of the observed responses were compared. Individual and aggregate factor coefficients and P-values demonstrated the effect of each component on chosen replies. The relevance of the chosen model and other factors examined by ANOVA was also revealed by the P-value (Table 4). The model terms were judged to be significant, and the lack of fit was not significant for any observed response, as predicted. Table 3 displays the 17 runs of the experimental design, as well as the outcomes of each run. Figures 4, 5, and 6 show 3D response surface plots of all responses to highlight the effects of various settings. Statistical analysis, calculated p-values and the fitting mathematical model provide the results of discrete main effects and their interaction factors with 95% confident level.

Table 3. Generated table of formulation composition and the effect on different formulation variables.

Samples	Variables			Responses		
Experimental Run	Drug conc. (X_1)	Surfactant conc. (X_2)	Solid lipid conc. (X_3)	PS (Y_1)	ZP (Y_2)	EE (Y_3)
1	0	0	0	375.2 ± 2.7	−35.6 ± 0.24	80 ± 2.14
2	0	0	0	375.3 ± 2.9	−35.1 ± 0.18	85 ± 2.22
3	−1	−1	0	352.1 ± 2.6	−36.4 ± 0.32	86 ± 1.10
4	−1	0	−1	356.6 ± 1.9	−35.7 ± 0.28	74 ± 1.23
5	0	1	1	371.4 ± 3.1	−37.2 ± 0.23	83 ± 2.30
6	0	−1	−1	375.1 ± 1.5	−36.2 ± 0.39	76 ± 1.94
7	−1	1	0	350.1 ± 2.5	−37.8 ± 0.28	82 ± 1.85
8	0	0	0	376.3 ± 2.7	−35.9 ± 0.32	86 ± 2.36
9	0	−1	1	372.1 ± 3.4	−38.5 ± 0.36	64 ± 2.17
10	1	1	0	379.8 ± 2.6	−37.1 ± 0.26	84 ± 2.05
11	1	0	1	383.5 ± 3.2	−35.6 ± 0.14	72 ± 2.12
12	1	−1	0	385.7 ± 2.3	−37.2 ± 0.36	85 ± 2.33
13	0	0	0	374.6 ± 2.4	−35.2 ± 0.22	79 ± 1.34
14	−1	0	1	354.1 ± 2.9	−35.9 ± 0.17	71 ± 1.68
15	0	1	−1	378.5 ± 1.3	−37.5 ± 0.25	72 ± 1.53
16	1	0	−1	392.2 ± 1.8	−35.2 ± 0.19	75 ± 2.26
17	0	0	0	377.3 ± 2.3	−35.8 ± 0.13	81 ± 2.11

Table 4. Summary of results of regression analysis for responses Y_1, Y_2 and Y_3.

Parameter	PS (Y_1)	P-value	ZP (Y_2)	P-value	EE (Y_3)	P-value
Intercept	277.92	<0.0001	1.72	0.0021	62.91	0.0255
X_1	2305.20	<0.0001	0.0612	0.5460	1.12	0.7784
X_2	56.71	0.0004	0.8450	0.0506	6.13	0.5169
X_3	0.6613	0.5199	0.2112	0.2773	12.50	0.3621
X_1 X_2	9.61	0.0364	0.0100	0.8051	0.0000	1.0000
X_1 X_3	3.24	0.1775	0.5625	0.0960	2.25	0.6915
X_2 X_3	4.20	0.1315	1.69	0.0126	132.25	0.0157
X_1^2	97.31	<0.0001	0.0221	0.7143	1.78	0.7239
X_2^2	1.88	0.2915	0.0979	0.4489	408.52	0.0008
X_3^2	19.15	0.0082	11.85	<0.0001	8.25	0.4543

The response increases when a factor is preceded by a positive sign, whereas the response declines when the factor is preceded by a negative sign. In regression equations, interaction terms or quadratic relationships are indicated by multiple factors or higher-order terms, respectively. Non-linearity between factors and responses has also been suggested. A factor can yield a different degree of response when it is varied at different levels or when multiple factors are concurrently varied. Table 5 present response generated by Design Expert®. Final regression equation of the applied quadratic model for individual responses, viz., particle size (Y_1), zeta potential (Y_2) and entrapment efficiency (Y_3) generated by response surface methodology with Design Expert® software are given below.

Based on the quadratic order and polynomial model, response surface analysis were plotted as Figures 4, 5, and 6 in a three-dimensional model, representing the effect of various independent factors on the observed responses of particle size, zeta potential and entrapment efficiency respectively.

3.3.1. Effect on particle size

The particle size, PDI and zeta potential of various NLC formulations and encapsulation efficiency of FIN loaded NLCs immediately after preparation are displayed in Table 3. The mean diameter of particles was observed to be below 400 nm ranging 350.1 ± 2.5 nm (sample 7) to 392.2 ± 1.8 nm (sample 16) and PDI values were less than 0.305 indicative of narrow size distribution at the selected levels of variables, while the mean particle size was 372.79 nm, shown in Table 4 which is the intercept of the model.

Quadratic equation aspect of particle size generated from ANOVA:

$$\mathbf{Y_1 = 375.74 + 16.97{*}X_1 - 2.66{*}X_2 + 0.2875{*}X_3 - 1.55{*}X_1X_2 + 0.9000{*}X_1X_3^{*} - 1.03{*}X_2X_3 - 4.81{*}X_1^{2} + 0.6675{*}X_2^{2} - 2.13{*}X_3^{2}}$$

The amount of drug (X_1) and the amount of solid lipid (X_2) are the two most important elements that influence particle size ($p < 0.05$). Amount of solid lipid had a negative effect on particle size. A reduced amount of solid lipid may encourage formation and subsequent stabilization of smaller particles. It has been observed that with an increment in the oil (liquid lipid) content, there is a fall in the mean particle size of NLC. The surfactant with its potential to stabilize formulation also plays a critical role in the particle size [43].

Hu *et al.* 2005 also reported that addition of liquid lipid to formulation decreases viscosity inside NLC and also reduces the surface tension to form smaller particles. Addition of liquid lipid in NLC production can be dispersed in a lipid matrix and reduce particle size [44]. The drug concentration has a positive effect, owing to the increase in molecular density in the inner phase. According to the significant effect of variables on particle size, correlation coefficient is good and high as expected ($R^2 = 0.9960$).

3.3.2. Zeta potential analysis

The zeta potential of the NLC formulations ranged from −35.1 mV (sample 2) to −38.5 mV (sample 9) (Table 3), with the mean being −36.35 mV as per the model intercept (Table 4). The only independent factor that seems to influence is the interaction between amount of solid liquid and surfactant (X_2X_3). The zeta potential value shows an increment with an increase in the solid lipid-surfactant concentration (P-value 0.05).

Quadratic equation aspect of zeta potential generated from ANOVA:

$$\mathbf{Y_2 = -35.52000 + 0.087500{*}X_1 - 0.325000{*}X_2 - 0.162500{*}X_3 - 0.050000{*}X_1X_2 + 0.375000{*}X_1X_3^{*} + 0.650000{*}X_2X_3 + 0.072500{*}X_1^{2} - 0.152500{*}X_2^{2} - 1.67750{*}X_3^{2}}$$

This phenomenon may be attributed to the adsorption of soya lecithin over the exterior surface of NLCs. Soya lecithin was chosen as a lipophilic surfactant in the formulation over other surfactants suitable for topical applications as it increased the zeta-potential of NLCs that translated into their enhanced stability. The same behaviour may be achieved when these two factors interacted i.e., increment in the amount of lipid (X_2) or the amount of surfactant (X_3).

3.3.3. Entrapment efficiency (EE)

The percentage of FIN entrapped within the NLCs ranged from 65% (sample 9) to 86% (sample 8) (Table 3). According to Table 3 the average % EE was found 78.53 %. %EE is mainly affected by the solid lipid concentration (X_2), and lipid-surfactant mixture (X_1X_2). The high %EE may be related to Compritol ATO 888's hydrophobicity, which is linked to flaws in its lattice that provide space for active ingredients [45]. It's

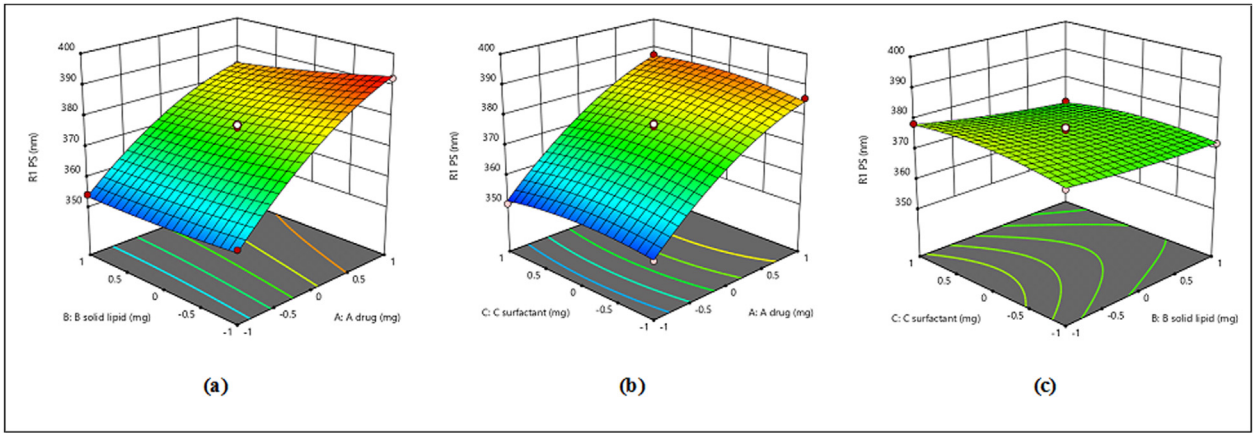

Figure 4. 3D response surface plot for effect of solid lipid – drug (a), surfactant – drug (b), and surfactant – solid lipid (c) concentration interaction terms on particle size.

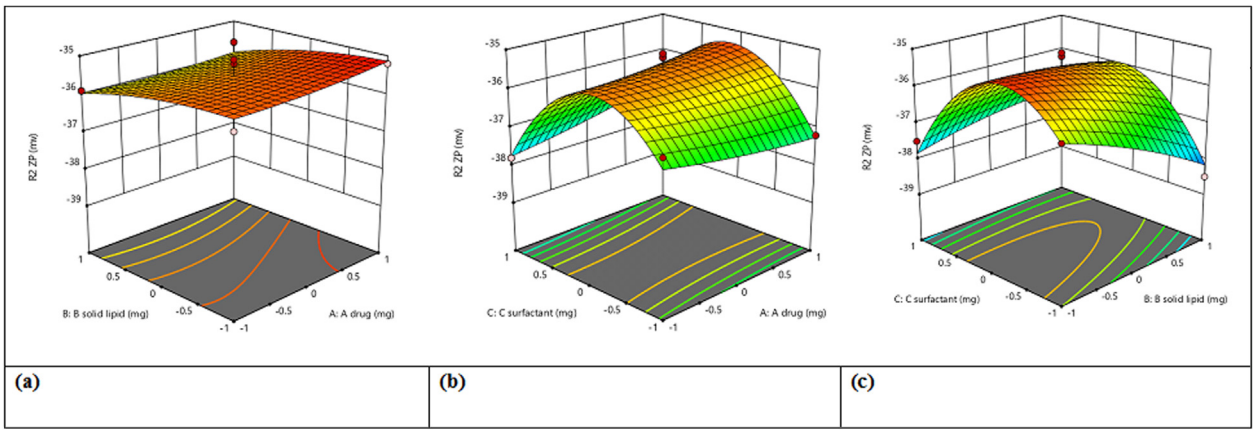

Figure 5. 3D response surface plot for effect of solid lipid – drug (a), surfactant – drug (b) and surfactant – solid lipid (c) concentration interaction terms on zeta potential.

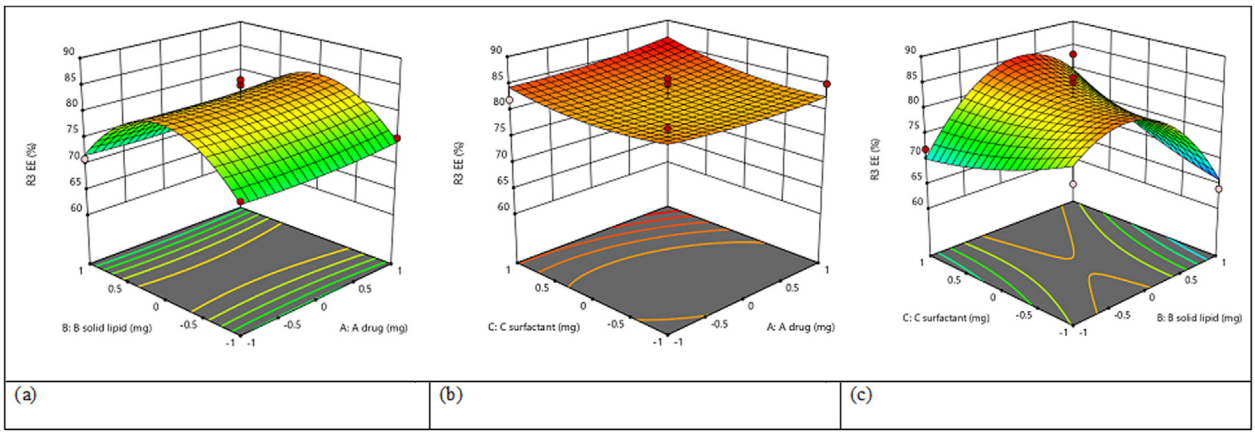

Figure 6. 3D response surface plot for effect of solid lipid – drug (a), surfactant – drug (b) and surfactant – solid lipid (c) concentration interaction terms on entrapment efficiency.

worth remembering that such a large drug load could be due to the FIN's lipophilic characteristics, and it having log P-value as 3.03 [46].

Quadratic equation aspect of entrapment efficiency generated from ANOVA:

$$Y_3 = 80.80000 + 0.375000*X_1 - 0.875000*X_2 + 1.25000*X_3 - 1.42630E - 14*X_1X_2 + 0.750000*X_1X_3 + 5.75000*X_2X_3 + 1.35000*X_1^2 - 9.15000*X_2^2 + 2.10000*X_3^2$$

Studies demonstrate that integration of liquid lipids into solid lipid causes disorder in solid lipid crystal, thereby permitting additional space to accommodate drug molecules. Surfactant molecules, in general, cover the distributed NLCs' hydrophobic interface. A large fraction of the drug molecules will be trapped within the surfactant layer on the exterior of NLCs with a greater surfactant concentration, resulting in a high EE [26,47].

3.4. Optimization and validation

Desirability function of Design Expert-11 was employed to get the optimized formulation. Since, the ZP was always around −35 mV, the desired value (<0.2), the formulation optimization was conducted with respect to particle size (~380 nm) and entrapment efficiency (maximum). Following the evaluation of numerous responses and a thorough search using desirability function, the optimal formulation (i.e. formulation no. 10) met the standards of optimised formulations.

Table 5. Responses generated through Design Expert.

Response	Unit	Min.	Max.	Mean	Std. Dev.	Ratio	Model
R_1	nm	350.1	392.2	372.79	12.53	1.12	Quadratic
R_2	mV	−38.5	−35.1	−36.35	1.02	1.10	Quadratic
R_3	%	64	86	78.53	6.41	1.34	Quadratic

3.5. Morphological properties

Transmission electron microscopic studies indicated that FIN loaded NLCs were spherical with a narrow size distribution and aggregation-free

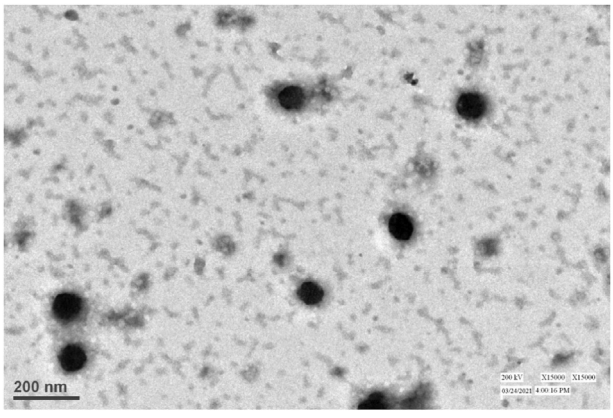

Figure 7. Transmission electron microscopy of FIN loaded NLCs.

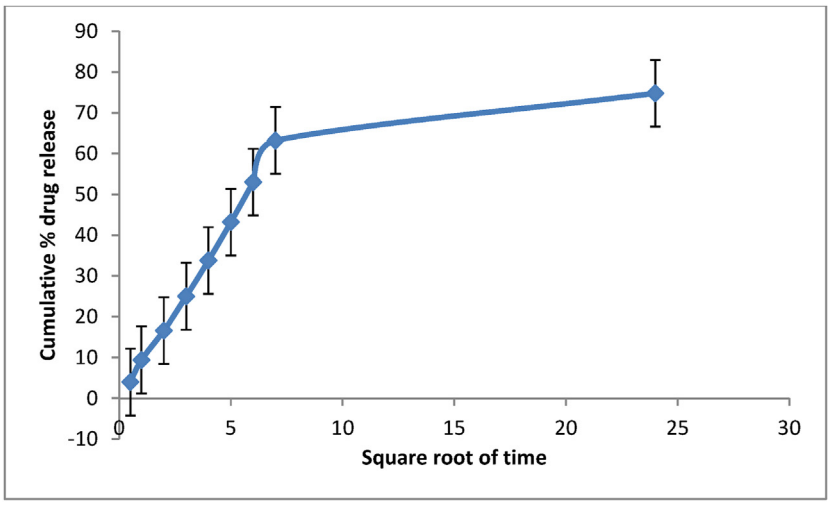

n=3

Figure 8. Drug release profile of NLC formulation.

(Figure 7). The observed particle diameters (c.a. 250 nm) were in agreement with the values attained from particle size analyzer.

3.6. Drug release

One of the key objectives of activation regarding formulation is to control the drug release from the nano-systems. The *in vitro* release profile curves over 24 h were obtained by the modified Franz-diffusion cell method from FIN loaded NLC, plain drug dispersion and commercially available topical formulation of FIN. FIN loaded NLCs released the drug within 12 h, as illustrated in Figure 8. The release of FIN from the NLC was biphasic, with an initial faster release rate from the start till the fifth hour, which could be attributed to the free drug in the NLCs or surface-associated drug. This was followed by a slower release from the solid lipid core of NLCs shortly after and because of its considerably more lipophilic nature, FIN is reported to here to have a higher affinity for the lipid matrix [48].

The *in vitro* release data indicated a Higuchi diffusion release model with the best match R^2 value (0.848) in comparison to other kinetic models after assessing the release data of the drug-loaded NLCs by multiple kinetic models (Table 6). Based on Fickian diffusion, this model elucidates the time-dependent drug release from an insoluble matrix.

The preparation of NLCs involved its cooling from an elevated temperature to room temperature. This step promotes the concentration of the drug within the external layers of the particles, its superficial trapping and burst release. The release of FIN contained deep within the nanoparticles can last for up to 24 h. Furthermore, following lipid crystallisation, the solubility of oil in solid lipid is surpassed and as a result, oil precipitates, with the production of fine oil droplets embedded in solid lipid, leading to prolonged release. The observed release patterns may be useful for follicular application since the initial release may serve to improve the drug penetration, while subsequent steady release may provide the drug over an extended time frame [23, 49, 50, 51].

3.7. Stability study

The particle size may serve as a potential tool to determine the stability profile of the NLCs. Physical stability was determined by observing changes in particle size, PDI and zeta potential of NLCs stored at 6° and 25 °C. Alterations in particle dimensions are considered as indicator of formulation instability [27, 52]. None of the samples indicated particle aggregation through visual observations, for a period of 4 weeks. These studies suggested that FIN-laden NLCs were stable over this period with no significant change in the mean particle size and PDI. Broadly, NLCs were stable after 4 weeks with average particle size between 370 and 380 nm, PDI below 0.3 and EE remained over 85% during this period. At the end of this study period, the formulation exhibited macroscopic phase separation at both temperatures. Nanocarriers were produced at elevated temperature and subsequently rapidly cooled to 0 °C, thus there are greater chances of formation of alpha modification crystals; while during storage, this crystal change is to the more stable beta modification.

Table 6. R^2 values of different releasing models.

Zero order	First order	Korsemeyer-Peppas	Higuchi kinetics
0.660	0.426	0.540	0.848

4. Conclusion

In this study, NLCs with the potential for follicular targeting of FIN were successfully developed by microemulsion method and optimized by Box–Behnken design. With 17 runs generated through factorial design, the resultant polynomial equations and response surface plots, the optimum formulation with the desired properties could be prepared. On the basis of data it could be concluded that the amount of drug, lipid and surfactant used were critical factors for the production of FIN loaded NLCs that had a substantial influence on their physical attributes. This factorial design study have served as a valuable tool for optimizing NLC formulation for delivery of FIN.

FTIR analysis confirmed the effective entrapment of FIN within NLCs. DSC thermograms confirmed the presence of amorphous FIN within the optimized NLC formulation. The stability tests conducted over 4 weeks at 6° and 25 °C gave a good indication that the formulation could retain their primary attributes. *In vitro* release profile of FIN from NLCs indicated sustained release at the skin environment, however, with a biphasic drug release profile with initial burst release followed by sustained release. Thus, the optimized formulation may be suitable for topical administration. These lipid colloidal carriers show interesting properties for delivering FIN. On the basis of experimental results, it can be deduced that particle size, zeta potential and entrapment efficiency of the NLCs are suitable for follicular targeting. The current study confirmed that FIN loaded NLCs may be a potential carrier for topical administration of actives in the therapy of pilosebaceous related diseases. The topical delivery of FIN to the skin targets with NLCs could possibly serve to minimize its systemic absorption and associated adverse events.

Declarations

Author contribution statement

Shweta Ramkar: Performed the experiments; Analyzed and interpreted the data; Contributed reagents, materials, analysis tools or data; Wrote the paper.

Preeti K. Suresh: Conceived and designed the experiments; Analyzed and interpreted the data; Contributed reagents, materials, analysis tools or data.

Funding statement

This work was supported by Pt. Ravishankar Shukla University Research Scholarship [797/Fin./Sch./2021].

Data availability statement

Data included in article/supp. material/referenced in article.

Declaration of interest's statement

The authors declare no conflict of interest.

Additional information

No additional information is available for this paper.

Acknowledgements

One of the authors (SR) is thankful to Pt. Ravishankar Shukla University, Raipur for providing the Research Scholarship (797/Fin./Sch./2021). The authors would like to acknowledge the University Institute of Pharmacy, Pt. Ravishankar Shukla University, Raipur (Chhattisgarh) and the National Center for Natural Resources, Pt. Ravishankar Shukla University, Raipur (Chhattisgarh) for providing facilities to carry out this study. Authors wish to extend gratitude to The Department of Pharmaceutical Engineering and Technology (Formerly Department of Pharmaceutics), Banaras Hindu University, Varanasi for providing DSC and FTIR facility.

References

[1] M. Bienová, R. Kučerová, M. Fiuráśková, M. Hajdúch, Z. Kolář, Androgenetic alopecia and current methods of treatment, Acta Dermatovenerol. Alpina Pannonica Adriatica 14 (1) (2005) 5–8.
[2] L. Laino, A case of hair regrowth in a patient with complete androgen insensitivity syndrome and female pattern hair loss, J. Clin. Cosmet. Dermatol. 4 (1) (2020) 1–5.
[3] H.C. Huang, H. Lin, M.C. Huang, Lactoferrin promotes hair growth in mice and increases dermal papilla cell proliferation through Erk/Akt and Wnt signaling pathways, Arch. Dermatol. Res. 311 (5) (2019) 411–420.
[4] S. Ramkar, A.K. Sah, N. Bhuwane, I. Choudhary, N. Hemnani, Nano-lipidic carriers as a tool for drug targeting to the pilosebaceous units, Curr. Pharmaceut. Des. 26 (2020) 1–18.
[5] T. Madheswaran, R. Baskaran, R.K. Thapa, J.Y. Rhyu, H.Y. Choi, J.O. Kim, et al., Design and in vitro evaluation of finasteride-loaded liquid crystalline nanoparticles for topical delivery, AAPS PharmSciTech 14 (1) (2013) 45–52.
[6] E.R. Coskuner, B. Ozkan, M.G. Culha, Sexual problems of men with androgenic alopecia treated with 5-alpha reductase inhibitors, Sexual Med. Rev. 7 (2) (2019) 277–282.
[7] D. Monti, S. Tampucci, S. Burgalassi, P. Chetoni, C. Lenzi, A. Pirone, et al., Topical formulations containing finasteride . Part I: in vitro permeation/penetration study and in vivo pharmacokinetics in hairless rat, J. Pharmaceut. Sci. 103 (8) (2014) 2307–2314.
[8] M. Tabbakhian, N. Tavakoli, M. Reza, S. Daneshamouz, Enhancement of follicular delivery of finasteride by liposomes and niosomes. 1. In vitro permeation and in vivo deposition studies using hamster flank and ear models, Int. J. Pharmceut. 323 (1–2) (2006) 1–10.
[9] M. Caserini, M. Radicioni, C. Leuratti, O. Annoni, A novel finasteride 0.25% topical solution for androgenetic alopecia: pharmacokinetics and effects on plasma androgen levels in healthy male volunteers, Int. J. Clin. Pharm. Ther. (7) (2014) 1–8.
[10] H.M. Almeida, H.M. Cabral, Physicochemical characterization of finasteride: PEG-6000 and finasteride: Kollidon K25 solid dispersions, and finasteride: β-cyclodextrin inclusion complexes, J. Inclusion Phenom. Macrocycl. Chem. 70 (2011) 397–406.
[11] K.K. Sarwa, B. Mazumder, P.K. Suresh, C.D. Kaur, Topical analgesic nanolipid vesicles formulation of capsaicinoids extract of Bhut Jolokia (Capsicum chinense Jacq): pharmacodynamic evaluation in rat models and acceptability studies in human volunteers, Curr. Drug Deliv. 13 (8) (2016) 1325–1338.
[12] B. Subramaniam, Z.H. Siddik, N.H. Nagoor, Optimization of nanostructured lipid carriers: understanding the types, designs, and parameters in the process of formulations, J. Nanoparticle Res. 22 (141) (2020) 1–29.
[13] P. Vargas-Mora, D. Morgado-Carrasco, Spironolactone in dermatology: uses in acne, Hidradenitis Suppurativa , female pattern hair loss, and Hirsutism, Actas Dermo-Sifiliográficas 111 (8) (2020) 639–649.
[14] M. Haider, S.M. Abdin, L. Kamal, G. Orive, Nanostructured lipid carriers for delivery of chemotherapeutics: a review, Pharmaceutics 12 (288) (2020) 1–26.
[15] T.A. Ahmed, K.M. El-say, Transdermal film-loaded finasteride microplates to enhance drug skin permeation: two-step optimization study, Eur. J. Pharmaceut. Sci. 88 (2016) 246–256.
[16] M.M. Irfan, S.U. Shah, I.U. Khan, M.U. Munir, N.R. Khan, K.U. Shah, et al., Physicochemical characterization of finasteride nanosystem for enhanced topical delivery, Int. J. Nanomed. 16 (2021) 1207–1220.
[17] S.M. Soleymani, A. Salimi, Enhancement of dermal delivery of finasteride using microemulsion systems, Adv. Pharmaceut. Bull. 9 (4) (2019) 1–9.
[18] M.Z.U. Khan, S.A. Khan, M. Ubaid, A. Shah, R. Kousar, G. Murtaza, Finasteride topical delivery systems for androgenetic alopecia, Curr. Drug Deliv. 15 (8) (2018) 1100–1111.
[19] S.M.M. Moghddam, A. Ahad, M. Aqil, S.S. Imam, Y. Sultana, Optimization of nanostructured lipid carriers for topical delivery of nimesulide using Box–Behnken design approach, Artif. Cell Nanomed. Biotechnol. 45 (3) (2017) 617–624.
[20] S. Honary, P. Ebrahimi, M. Nikbakht, Optimization of finasteride nano-emulsion preparation using chemometric approach, Trop. J. Pharmaceut. Res. 12 (4) (2013) 457–460.
[21] B. Biruss, R. Dietl, C. Valenta, The influence of selected steroid hormones on the physicochemical behaviour of DPPC liposomes, Chem. Phys. Lipids 148 (2007) 84–90.
[22] N. Sethuraman, S. Shanmuganathan, K. Sandhya, B. Anbarasan, Design, development and characterization of nano structured lipid carrier for topical delivery of aceclofenac, Indian J. Pharmaceut. Educ. Res. 52 (4) (2018) 581–586.
[23] S.A. Swidan, Z.N. Mansour, Z.A. Mourad, N.A. Elhesaisy, N.A. Mohamed, M.S. Bekheet, et al., DOE, formulation, and optimization of Repaglinide nanostructured lipid carriers, J. Appl. Pharmaceut. Sci. 8 (10) (2018) 8–16.
[24] J. Pardeike, A. Hommoss, R.H. Müller, Lipid nanoparticles (SLN, NLC) in cosmetic and pharmaceutical dermal products, Int. J. Pharm. 366 (1–2) (2009) 170–184.
[25] M. Kim, K. Kim, S. Sohn, J. Lee, C.H. Lee, B.K. Lee, et al., Formulation and evaluation of nanostructured lipid carriers (NLCs) of 20 (S)-Protopanaxadiol (PPD) by Box-Behnken Design, Int. J. Nanomed. 14 (2019) 8509–8520.
[26] R.N. Shamma, M.H. Aburahma, Follicular delivery of spironolactone via nanostructured lipid carriers for management of alopecia, Int. J. Nanomed. 9 (1) (2014) 5449–5460.
[27] I.C. Id, M. Yasir, M. Verma, A.P. Singh, Nanostructured lipid carriers: a groundbreaking approach for transdermal drug delivery, Tabriz Univ. Med. Sci. 10 (2) (2020) 150–165.
[28] Y. Rao, F. Zheng, X. Zhang, J. Gao, W. Liang, In vitro percutaneous permeation and skin accumulation of finasteride using vesicular ethosomal carriers, AAPS PharmSciTech 9 (3) (2008) 860–865.
[29] P.I. Siafaka, N. Üstündağ Okur, E. Karavas, D.N. Bikiaris, Surface modified multifunctional and stimuli responsive nanoparticles for drug targeting: current status and uses, Int. J. Mol. Sci. 17 (9) (2016) 1–40.
[30] A. Kumar, V. Kushwaha, P.K. Sharma, Pharmaceutical microemulsion: formulation, characterization and drug deliveries across skin, Int. J. Drug Dev. Res. 6 (1) (2014) 1–21.
[31] A. Akhoond Zardini, M. Mohebbi, R. Farhoosh, S. Bolurian, Production and characterization of nanostructured lipid carriers and solid lipid nanoparticles containing lycopene for food fortification, J. Food Sci. Technol. 55 (1) (2018) 287–298.
[32] M. Ferreira, L.L. Chaves, A. Costa, S. Reis, Optimization of nanostructured lipid carriers loaded with methotrexate: a tool for inflammatory and cancer therapy, Int. J. Pharm. 492 (2015) 65–72.
[33] S.A. Wani, P. Kumar, Fenugreek: a review on its nutraceutical properties and utilization in various food products, J. Saudi Soc. Agric. Sci. 17 (2) (2018) 97–106.
[34] L.V. Roque, I.S. Dias, N. Cruz, A. Rebelo, A. Roberto, P. Rijo, et al., Design of finasteride-loaded nanoparticles for potential treatment of alopecia, Skin Pharmacol. Physiol. 30 (4) (2017) 197–204.
[35] P. Jaiswal, B. Gidwani, A. Vyas, Nanostructured lipid carriers and their current application in targeted drug delivery, Artif. Cell Nanomed. Biotechnol. 44 (1) (2016) 27–40.
[36] K.S. Ahmed, S.A. Hussein, A.H. Ali, S.A. Korma, Q. Lipeng, C. Jinghua, Liposome: composition, characterisation, preparation, and recent innovation in clinical applications, J. Drug Target. 27 (7) (2019) 742–761.
[37] A. Puri, K. Loomis, B. Smith, J.H. Lee, A. Yavlovich, E. Heldman, et al., Lipid-based nanoparticles as pharmaceutical drug carriers: from concepts to clinic, Crit. Rev. Ther. Drug Carrier Syst. 26 (6) (2009) 523–580.
[38] R.N. Shamma, M.H. Aburahma, Follicular delivery of spironolactone via nanostructured lipid carriers for management of alopecia, Int. J. Nanomed. 9 (1) (2014) 5449–5460.

[39] S. Mardiyanto, Investigation of Nanoparticulate Formulation Intended for Caffeine Delivery to Hair Follicles, Dissertation, Universitat des Saarlandes, 2013, pp. 13–30.
[40] O.A.A. Ahmed, W.Y. Rizq, Finasteride nano-transferosomal gel formula for management of androgenetic alopecia: ex vivo investigational approach, Drug Des. Dev. Ther. 12 (2018) 2259–2265.
[41] T.A. Ahmed, Preparation of finasteride capsules-loaded drug nanoparticles: formulation, optimization, in vitro, and pharmacokinetic evaluation, Int. J. Nanomed. 11 (2016) 515–527.
[42] S. Sujatha, G. Sowmya, M. Chaitanya, V.S.K. Reddy, M. Monica, K.K. Kumar, Preparation, characterization and evaluation of finasteride ethosomes, Int. J. Drug Deliv. Technol. 8 (1) (2016) 1–11.
[43] J. Das Neves, B. Sarmento, Precise engineering of dapivirine-loaded nanoparticles for the development of anti-HIV vaginal microbicides, Acta Biomater. 18 (February) (2015) 77–87.
[44] F.Q. Hu, S.P. Jiang, Y.Z. Du, H. Yuan, Y.Q. Ye, S. Zeng, Preparation and characterization of stearic acid nanostructured lipid carriers by solvent diffusion method in an aqueous system, Colloids Surf. B Biointerfaces 45 (3–4) (2005) 167–173.
[45] Y. Zhai, G. Zhai, Advances in lipid-based colloid systems as drug carrier for topic delivery, J. Contr. Release 193 (2014) 90–99.
[46] T.A. Ahmed, Preparation of finasteride capsules-loaded drug nanoparticles: formulation, optimization, in vitro, and pharmacokinetic evaluation, Int. J. Nanomed. 11 (2017) 515–527.
[47] W. Wang, L. Chen, X. Huang, A. Shao, Preparation and characterization of minoxidil loaded nanostructured lipid carriers, AAPS PharmSciTech 18 (2) (2017) 509–516.
[48] K.R. Vimal, V. Sankar, C.R. Srinivas, M. Kumaresan, Enhancement of folicular delivery of finasteride in niosomal and proniosomal gel form for treating androgenetic alopecia, Indian Drugs 49 (5) (2012) 47–55.
[49] S.K. Jain, A. Verma, A. Jain, P. Hurkat, Transfollicular drug delivery: current perspectives, Res. Rep. Transdermal Drug Deliv. 5 (2016) 1–17.
[50] R. Kumar, B. Singh, G. Bakshi, O.P. Katare, Development of liposomal systems of finasteride for topical applications: design, characterization, and in vitro evaluation, Pharmaceut. Dev. Technol. 12 (2007) 591–601.
[51] C. Mathes, A. Melero, P. Conrad, T. Vogt, L. Rigo, D. Selzer, et al., Nanocarriers for optimizing the balance between interfollicular permeation and follicular uptake of topically applied clobetasol to minimize adverse effects, J. Contr. Release 223 (2016) 207–214.
[52] B. Heurtault, P. Saulnier, B. Pech, J.E. Proust, J.P. Benoit, A novel phase inversion-based process for the preparation of lipid nanocarriers, Pharmaceut. Res. 19 (6) (2002) 875–880.